Journal of Dental Sciences 18 (2023) 282–294

Available online at www.sciencedirect.com

ScienceDirect

journal homepage: www.e-jds.com

Original Article

Hsa_circ_0005050 regulated the progression of oral squamous cell carcinoma via miR-487a-3p/CHSY1 axis

Xubin Chen [a,1], Qiaojiang Chen [b,1], Chen Zhao [c], Zhiqi Lu [b*]

[a] *Department of Oral and Maxillofacial Surgery, Hainan General Hospital, Hainan Affiliated Hospital of Hainan Medical University, Haikou, China*
[b] *Department of Anesthesiology, Hainan General Hospital, Hainan Affiliated Hospital of Hainan Medical University, Haikou, China*
[c] *Department of Oral and Maxillofacial Surgery, Jiangmen Central Hospital, Jiangmen, China*

Received 11 April 2022; Final revision received 18 May 2022
Available online 4 June 2022

KEYWORDS
circ_0005050;
miR-487a-3p;
CHSY1;
OSCC

Abstract *Background/purpose:* Circular RNAs (circRNAs) have been identified as potential functional modulators of the cellular physiology processes. This study aims to learn the potential molecular mechanisms of hsa_circ_0005050 (circ_0005050) in oral squamous cell carcinoma (OSCC).
Materials and methods: Quantitative reverse transcriptase-polymerase chain reaction (qRT-PCR) was used to examine the expression of circ_0005050, miR-487a-3p, and chondroitin sulfate synthase 1 (CHSY1). Dual-luciferase reporter system, RNA pull-down, and RNA Immunoprecipitation (RIP) assays were used to determine the binding between miR-487a-3p and circ_0005050 or CHSY1. Colony formation experiment and EdU assay were used to investigate proliferation. Wound-healing and transwell assays were used to detect the migration of cells. The apoptosis rate of OSCC cells was tested by flow cytometry. Protein levels of related factors were determined by Western blot. Tumor xenograft was established to determine the regulatory role of circ_0005050 on tumor growth *in vivo*, and Ki-67 expression was detected in this xenograft using Immunohistochemical (IHC).
Results: We implicated that circ_0005050 was apparently upregulated in OSCC tissues cells. In function experiments, repressing of circ_0005050 remarkably retarded OSCC growth *in vitro*. Furthermore, we conducted dual-luciferase reporter assays and RNA pull-down assays to verify that circ_0005050 sponged miR-487a-3p. Suppression of miR-487a-3p rescued the inhibition of proliferation in SCC15 and SCC25 cells induced by circ_0005050 knockdown. In addition, we found that overexpression of CHSY1 also reversed the inhibitory effect of circ_0005050

* Corresponding author. Department of Anesthesiology, Hainan General Hospital, Hainan Affiliated Hospital of Hainan Medical University, No. 19, Xiuhua Road, Xiuying District, Haikou, 570311. China.
E-mail address: doctor12182021@163.com (Z. Lu).
[1] These two authors contributed equally to this work.

https://doi.org/10.1016/j.jds.2022.05.012

silencing on cell proliferation. Moreover, circ_0005050 knockdown inhibited tumor growth *in vivo*.
Conclusion: Circ_0005050 acted as an oncogenic factor in OSCC progression through miR-487a-3p/CHSY1 axis.

Introduction

Squamous cell carcinoma (SCC) is a kind of epithelial malignant tumor, characterized by numerous anatomical sites and remarkable metastases, SCC accounts for 90% of head and neck malignant tumors.[1,2] Oral squamous cell carcinoma (OSCC) is the most usual form of SCC of the head and neck.[3,4] The main treatment is surgery, radiotherapy, and chemotherapy.[5,6] Because the location of OSCC is often limited, and usually close to vital organs, such as important blood vessels, brain, neck, and upper respiratory tract, severely limits the operation scope; at the same time, the cause of maxillofacial surgery patients with large defect and functional defect directly affect the quality of life of SCC patients.[7,8] Therefore, despite many years of research, the pathogenesis of OSCC is not well understood. Therefore, it is very important to further explore the pathogenesis and potential molecular targets of OSCC.

CircRNA is a circular non-coding RNA molecule formed by covalently pairing. It does not have a free 5′ -end cap and 3′ -end poly tail.[9,10] The precursor RNA can be spliced directly into a loop, so it is not easy to be degraded by RNase R enzyme.[11] CircRNAs have also been implicated in various human diseases, such as cancer and autoimmune diseases, suggesting that circRNA may be novel tumor molecular markers or therapeutic targets.[12,13] In OSCC, *Zhu* et al. found that circ-PVT1 was highly expressed in OSCC, and it might sponge miR-106a-5p to regulate the expression level of related genes, and ultimately affect the proliferation ability of OSCC *in vivo* and *in vitro*.[14] Nevertheless, the action of circ_0005050 in OSCC is still unclear. This test was to probe the role of circ_0005050 on the evolution of OSCC.

MicroRNAs (miRNAs) are non-coding RNAs of 18–25 nucleotides in length, miRNAs regulate gene expression by binding to the 3′ untranslated regions (UTRs) of their target mRNAs through complementary interactions.[15] MiRNAs were found to be involved in cell proliferation, metastasis, differentiation, and autophagy, and their abnormal expression is involved in tumorigenesis and development.[16] *Zhang* et al. found that miR-105 expression level was notably boosted in OSCC tissues and cells, which might be involved in oral mucosa.[17] *Wang* et al. found that miR-487a-3p played an inhibitory role in the happenings and developments of OSCC.[18] However, the effect of circ_0005050 and miR-487a-3p on the mechanism of OSCC has not been reported.

Chondroitin sulfate synthase 1 (CHSY1) is one of the six enzymes responsible for the biosynthesis of chondroitin sulfate in mammalian cells, and its methylation level is related to T cell differentiation.[19] Recent consequences have revealed that CHSY1 is dysregulated in all kinds of tumors, such as osteosarcoma, renal clear cell carcinoma and colorectal cancer.[20] In addition, *Li* et al. found that the level of CHSY1 was evidently increased in OSCC cells and tissues.[21]

The objective of this work was to learn circ_0005050 expression in OSCC tissues and cells and its effect on the migration of OSCC, as well as the effect of circ_0005050 on OSCC through the miR-487a-3p/CHSY1 axis.

Materials and methods

Clinical tissue samples

OSCC tissues and adjacent tissues from Hainan General Hospital. This study was approved by the Ethics Committee of Hainan General Hospital. All patients were informed and signed consent forms. The detailed clinical characteristics of patients are described in Table 1.

Cell culture and transfection

All cells were obtained from Shanghai Enzyme Research Biotechnology Co., LTD (Shanghai, China). Human oral keratinocyte cells (HOK) and OSCC cells (SCC15, SCC25) were cultured in DMEM complete medium (90% DMEM+10% FBS) at 5% CO_2 and 37 °C.

Table 1 Correlation between clinicopathologic parameters of oral squamous cell carcinoma patients and circ_0005050 expression.

Parameter	Case	Circ_0005050 expression		*P* value
		Low (n = 23)	High (n = 24)	
Age (years)				0.654
≤60	25	13	12	
>60	22	10	12	
Gender				0.671
Female	21	11	10	
Male	26	12	14	
Tumor size				0.002*
≤5 cm	26	18	8	
>5 cm	21	5	16	
TNM stages				<0.0001*
I–II	21	17	4	
III	26	6	20	

TNM: tumor-node-metastasis; *$P < 0.05$.

The circ_0005050 small interference RNA (si-circ_0005050), miR-487a-3p mimic/inhibitor (miR-487a-3p, anti-miR-487a-3p), CHSY1 overexpression (pcDNA3.0-CHSY1), short hairpin-circ_0005050 (sh-circ_0005050), circ_0005050 overexpression (oe-circ_0005050), and their corresponding controls (si-NC, miR-NC, anti-miR-NC, pcDNA3.0-NC, sh-NC, and oe-NC) were designed and synthesized by Guangzhou Ruibo Biotechnology Co., LTD (Guangzhou, China), and were transfected into SCC15 and SCC25 cells by Lipofectamine3000 (Invitrogen, Paisley Scotland, UK), respectively. The operation was carried out strictly in accordance with the experimental instructions.

Quantitative reverse transcriptase-polymerase chain reaction (qRT-PCR)

Total RNA of tissues and cells was extracted and reversely transcribed into cDNA using PrimeScript™ RT Master Mix Kit (Takara, Tokyo, Japan). PCR was performed according to SYBR Green PCR (Takara) kit instructions. $2^{-\Delta\Delta Ct}$ method was used for calculating the relative expression level. β-actin and U6 were used as internal parameters. As shown in Table 2 are the primer sequences.

Colony formation assay

SCC15 and SCC25 cells at logarithmic growth stage were prepared into uniform cell suspensions and inoculated into petri dishes at a density of 1×10^3 for routine culture for about 14 days. Discarded the supernatant, added methanol and let stand for 15 min. Stained with crystal violet (Sigma—Aldrich, St. Louis, MO, USA) for 20 min and rinsed the remaining solution with PBS, and the number of clones was calculated using a microscope (Olympus, Tokyo, Japan; magnification × 40).

5-Ethynyl-2′-deoxyuridine (EdU) assay

The transfected SCC15 and SCC25 cells were inoculated with 5 × 103 cells into 96-well culture plates and cultured in an incubator. EdU medium was prepared according to the instructions of the EdU assay kit (RiboBio, Guangzhou, China), and cells were incubated with it, and the cells were labeled with EdU (50 μM, RiboBio) for 2 h at 37 °C. 4% formaldehyde solution fixture, Apollo staining, DNA staining and a microscope photographing were carried out in sequence according to the instructions.

Table 2 The sequences of primers for RT-qPCR[a] used in this study.

Name		Primers for PCR (5′-3′)
hsa_circ_0005050	Forward	TTTGATGCTGTTTTTGAATGCAC
	Reverse	AGTGTTCTTGTACTGTTT GATCTGT
CHSY1[b]	Forward	TTCACTTTTGCGCCAATCGC
	Reverse	CACATCCTCCGGCTTAGCTC
miR-487a-3p	Forward	GCCGAGAATCATACAGGGACAT
	Reverse	CTCAACTGGTGTCGTGGAG
β-actin	Forward	CTTCGCGGGCGACGAT
	Reverse	CCACATAGGAATCCTTCTGACC
U6	Forward	CTCGCTTCGGCAGCACA
	Reverse	AACGCTTCACGAATTTGCGT

[a] RT-qPCR: Quantitative reverse transcriptase polymerase chain reaction.
[b] CHSY1: chondroitin sulfate synthase 1.

OSCC cell migration experiment after transfection

The migration ability of cells was detected by scratch assay and Transwell assay. In the scratch experiment, the cells were inoculated in the Petri dish. When the degree of fusion reached more than 90%, the cells were scratched with the straw tip and cultured in serum-free medium for 24 h. The relative mobility was calculated according to the scratch area. In Transwell experiment, complete medium was added in the lower chamber and serum-free medium was inoculated in the upper chamber, while the bottom chamber was added with the medium containing 10% FBS. After 24 h, the film was fixed with 4% paraformaldehyde (Sigma—Aldrich), then stained with 0.1% crystal violet (Sigma—Aldrich) and photographed under a microscope.

Flow cytometry assay

A commercial Annexin V-FITC/PI Apoptosis kit (Bender Med System, Vienna, Austria) was applied to analyze cell apoptosis. In short, the transfected OSCC cells were digested and re-suspended, then inoculated into 6-well plates at a cell density of 5×10^4 per well cultivated for 24 h. Trypsin and DMEM culture medium were successively added for digestion and termination of digestion. PBS solution was repeatedly washed and centrifuged twice, and cells were resuspended to prepare mononuclear cell suspension with a density of 5×10^5. 500 μL binding buffer, 5 μL Annexin V-FITC, and 5 μL PI was added to each tube. Cells were protected from light for 15 min at room temperature. Then the cell apoptosis was detected by flow cytometry (BD Bioscience, San Jose, CA, USA).

Western blot assay

Total protein was extracted from RIPA lysis buffer (Beyotime, Shanghai, China) and quantified by BCA (Thermo Fisher Scientific, Rockford, IL, USA) method. The protein samples were loaded at 40 μg/well, and SDS-PAGE was performed. The protein was then transferred to PVDF membrane (Millipore. Bedford, MA, USA), which was sealed with 5% skim milk for 2 h and then incubated overnight with primary antibodies: PCNA (ab18197, 1:1000, Abcam, Cambridge, MA, USA), CDK6 (ab151247, 1:1000, Abcam), Bcl2 (ab32124, 1:1000, Abcam), Bax (ab182733, 1:1000, Abcam), CHSY1 (ab153813, 1:1000, Abcam), and β-actin (ab8227, 1:1000, Abcam) at 4 °C. On the second day, the membrane was washed with TBST solution 3 times, 10 min each time, and the second antibody (ab6721, 1:10000, Abcam) was incubated at room temperature for 1 h. Finally, ECL chemiluminescence (GE Healthcare UK Ltd, Little Chalfont, UK) was developed in a dark room.

Dual-luciferase reporter assay

Generally, the wild-type (WT) luciferase reporter constructs (circ_0005050-WT and CHSY1-3′UTR-WT) and the site-directed mutant (MUT) constructs (circ_0005050- MUT and CHSY1-3′UTR-MUT) were acquired from Hanbio (Shanghai, China). SCC15 and SCC25 cells in logarithmic growth phase were inoculated into 24-well plates, and when the cell convergence reached about 50%, they were co-transfected with circ_0005050-WT, circ_0005050-MUT, CHSY1-3′UTR-WT, CHSY1-3′UTR-MUT or miR-487a-3p and miR-NC, respectively. The results were determined by luciferase reporter gene detector (Promega, Madison, WI, USA).

RNA pull-down assay

In brief, SCC15 and SCC25 cells were transfected with biotinylated miRNA (Bio-miR-487a-3p) or Bio-miR-NC (50 nM) using Lipofectamine RNAiMax (Life Technologies, Carlsbad, CA, USA) for 48 h. Then, total RNA from the cells was harvested and extracted. 125 μL streptavidin magnetic beads were mixed with 25 μL probe solution at a final concentration of 8 μmol/L. The mixture of streptavidin beads and probe solution was lightly mixed with total RNA and incubated for 30 min at room temperature. Eluting buffer was added to collect the bound RNA complex. The level of circ_0005050 was detected by qRT-PCR.

RNA Immunoprecipitation (RIP) assay

In short, SCC15 and SCC25 cells at 80% confluency were harvested and lysed in complete RIP lysis buffer (Millipore). After that, the obtained cell extracts were mixed with RIP buffer and magnetic beads conjugated with anti-Argonaute2 (Ago2) antibody (Millipore) or normal mouse IgG (Millipore). After being digested and wash, total RNA was extracted for the measurement of miR-487a-3p and CHSY1 using qRT-PCR.

Tumor xenograft assay

Ten nude mice (Vital River Laboratory, Beijing, China) were randomly divided into two groups after adaptation culture. SCC15 cells stably transfected with sh-circ_0005050, oe-circ_0005050, sh-NC, or oe-NC were injected (1×10^6 cells/mice), and the size of the subcutaneous tumor was measured on day 7, 14, 21, 28 and 35, and tumor volume was calculated according to the formula: volume = length × width^2/2. Mice were sacrificed on day 35 after the size of subcutaneous tumor was measured, and the tumor weight was tested. The experiment was approved by the Animal Ethics Committee of the Hainan General Hospital.

Immunohistochemical (IHC) analysis

OSCC tissue was fixed with 10% formalin and then paraffin-embedded. Slices were incubated with anti-Ki-67 (ab16667, 1:200, Abcam) overnight at 4 °C, cleaned twice, and then incubated with a secondary antibody at room temperature. The samples were stained with 3, 3-diaminobenzidine solution and hematoxylin (Sigma–Aldrich). Finally, the slides were observed under a microscope.

Statistical analysis

Mean ± standard deviation was used for measurement data, and *t*-test was used for comparison between the two groups. Pearson correlation analysis was used to analyze the expression association. One-way ANOVA and Tukey's were used for data comparison between multiple groups. $P < 0.05$ indicated that the difference was statistically significant.

Results

Circ_0005050 was significantly up-regulated in OSCC tissues and cells

Circ_0005050 is a transcription product of the XPO1 gene located at chr2: 61712902–61717911. It includes four exons and has a spliced sequence length of 621 bp (Fig. 1A). We confirmed the higher levels of circ_0005050 in the OSCC tissues and cells relative to the normal group (Fig. 1B and C). To probe the association of circ_0005050 expression with the clinic-pathologic feature, all patients with OSCC were then classified in Table 1, based on the median value of circ_0005050. Results exhibited that circ_0005050 expression was associated with Tumor size and TNM stages. Overall, circ_0005050 was upregulated in OSCC.

Downregulation of circ_0005050 inhibited cell growth and migration

Si-circ_0005050 and si-NC were transfected into SCC15 and SCC25 cells, and the transfection efficiency was measured by qRT-PCR. The abundance of circ_0005050 was apparently impeded by transfected si-circ_0005050 into SCC15 and SCC25 cells (Fig. 2A). The relative colony number and EdU positive rate were decreased after circ_0005050 knockdown, confirming the attenuated proliferative capacity (Fig. 2B and C). Additionally, wound healing and transwell tests showed that the migratory ability of SCC15 and SCC25 cells were reduced after knocking down circ_0005050 (Fig. 2D and E). Next, flow cytometry assay elucidated that the apoptosis rate was strongly elevated by circ_0005050 knockdown (Fig. 2F). Western blot manifested that the expression of PCNA, CDK6 and Bcl2 was pronouncedly weakened by the downregulation of circ_0005050, while the expression of Bax was reinforced (Fig. 2G and H). In addition, our data suggested that the upregulation of circ_0005050 might obviously enhance the number of colonies in SCC15 and SCC25 cells (Fig. S1A and S1B). These consequences disclosed that circ_0005050 knockdown suppressed cell proliferation, and migration and promoted apoptosis.

Circ_0005050 functioned as a sponge of miR-487a-3p in OSCC cells

The circinteractome (https://circinteractome.nia.nih.gov/) algorithm provided a potential binding relationship between circ_0005050 and miR-487a-3p (Fig. 3A).

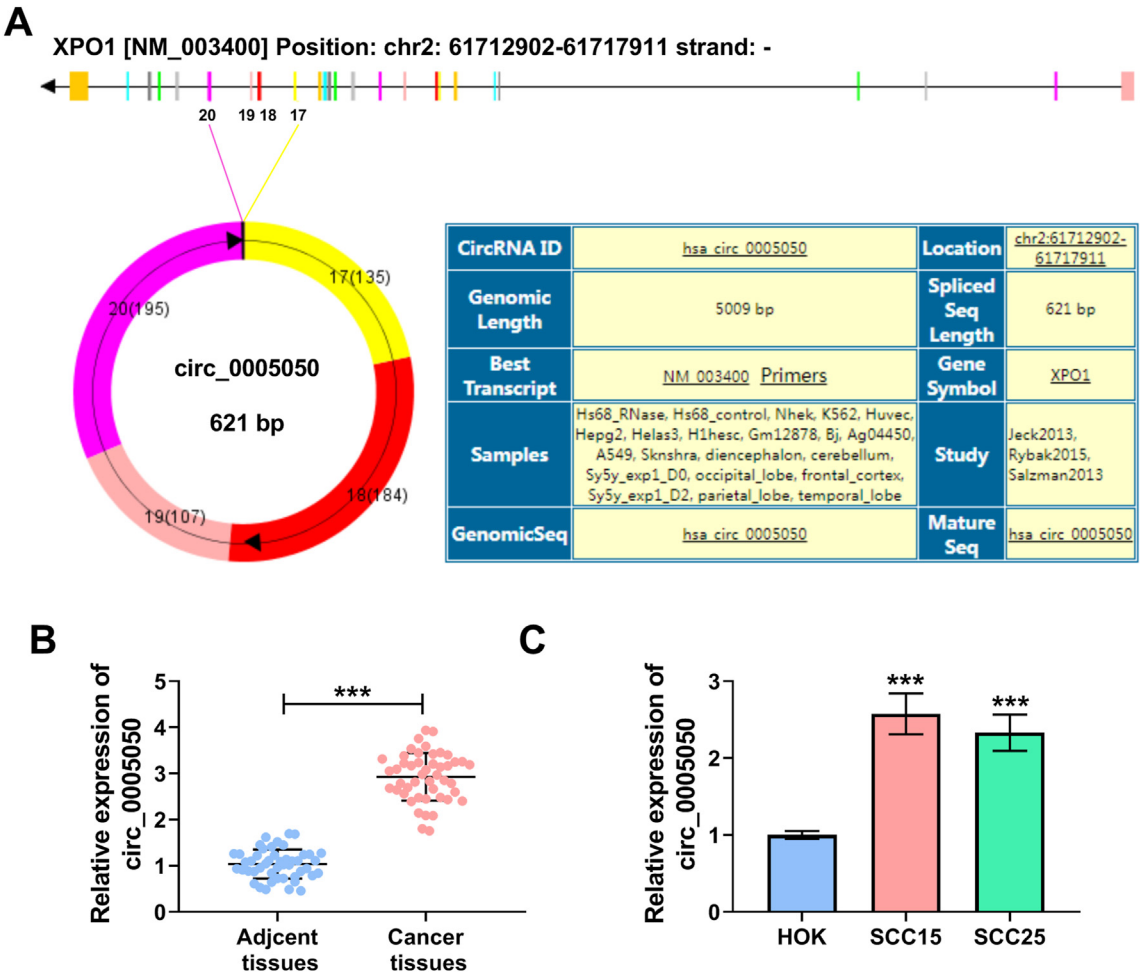

Fig. 1 The expression of circ_0005050 was overexpressed in OSCC tumor tissues and cell lines. (A) Circ_0005050 was composed of exon 17—20 of gene XPO1. (B) QRT-PCR revealed the level of circ_0005050 in OSCC tumor tissues and paired adjacent tissues. (C) QRT-PCR was applied to detect the expression level of circ_0005050 in human OSCC cell lines and normal human oral epithelial cell lines. ***$P < 0.001$.

Expression of miR-487a-3p was low expressed in OSCC tumor tissues and cells in contrast with normal group (Fig. 3B and C). Dual-luciferase reporter assay confirmed an attenuated luciferase activity of SCC-15 and SCC25 cells co-transfected with circ_0005050-WT and miR-487a-3p mimic, and a stable luciferase activity with co-transfection of circ_0005050-WT and miR-487a-3p mimic (Fig. 3D and E). RNA pull-down assay revealed enrichment of circ_0005050 in Bio-miR-487a-3p mediated precipitation (Fig. 3F and G). In addition, qRT-PCR analysis suggested that the expression level of miR-487a-3p was negatively correlated with circ_0005050 in OSCC tissues samples (Fig. S2A). These outcomes suggested miR-487a-3p as a target of circ_0005050.

Inhibition of miR-487a-3p regained the regulatory effects of circ_0005050 knockdown in OSCC cells

The efficiency of miR-487a-3p inhibition was evaluated, and we noticed that the expression of miR-487a-3p was strikingly diminished in SCC15 and SCC25 cells with anti-miR-487a-3p transfection relative to anti-miR-NC (Fig. 4A). Of note, cell proliferation, impeded by si-circ_0005050, was overturned in SCC15 and SCC25 cells transfected with si-circ_0005050+anti-miR-487a-3p (Fig. 4B and C). Likewise, cell migration, hindered by circ_0005050 silencing alone, was relieved by anti-miR-487a-3p (Fig. 4D and E). The apoptosis rate was facilitated in SCC15 and SCC25 cells transfected with si-circ_0005050 but obviously blocked in cells transfected with si-circ_0005050+anti-miR-487a-3p (Fig. 4F). Additionally, the expression of PCNA, CDK6 and Bcl2 was decreased in cells transfected with si-circ_0005050 but expedited in cells transfected with si-circ_0005050+anti-miR-487a-3p, while the expression of Bax was opposite to these proteins expressed in these transfection groups (Fig. 4G and H). Above data presented that circ_0005050 knockdown exerted roles by inducing the expression of miR-487a-3p.

CHSY1 was a downstream target of miR-487a-3p

According to starBase (http://starbase.sysu.edu.cn/), there were potential complementary binding sites of miR-487a-3p and CHSY1 3′UTR (Fig. 5A). Expression of CHSY1 at mRNA level and protein level was elevated in OSCC

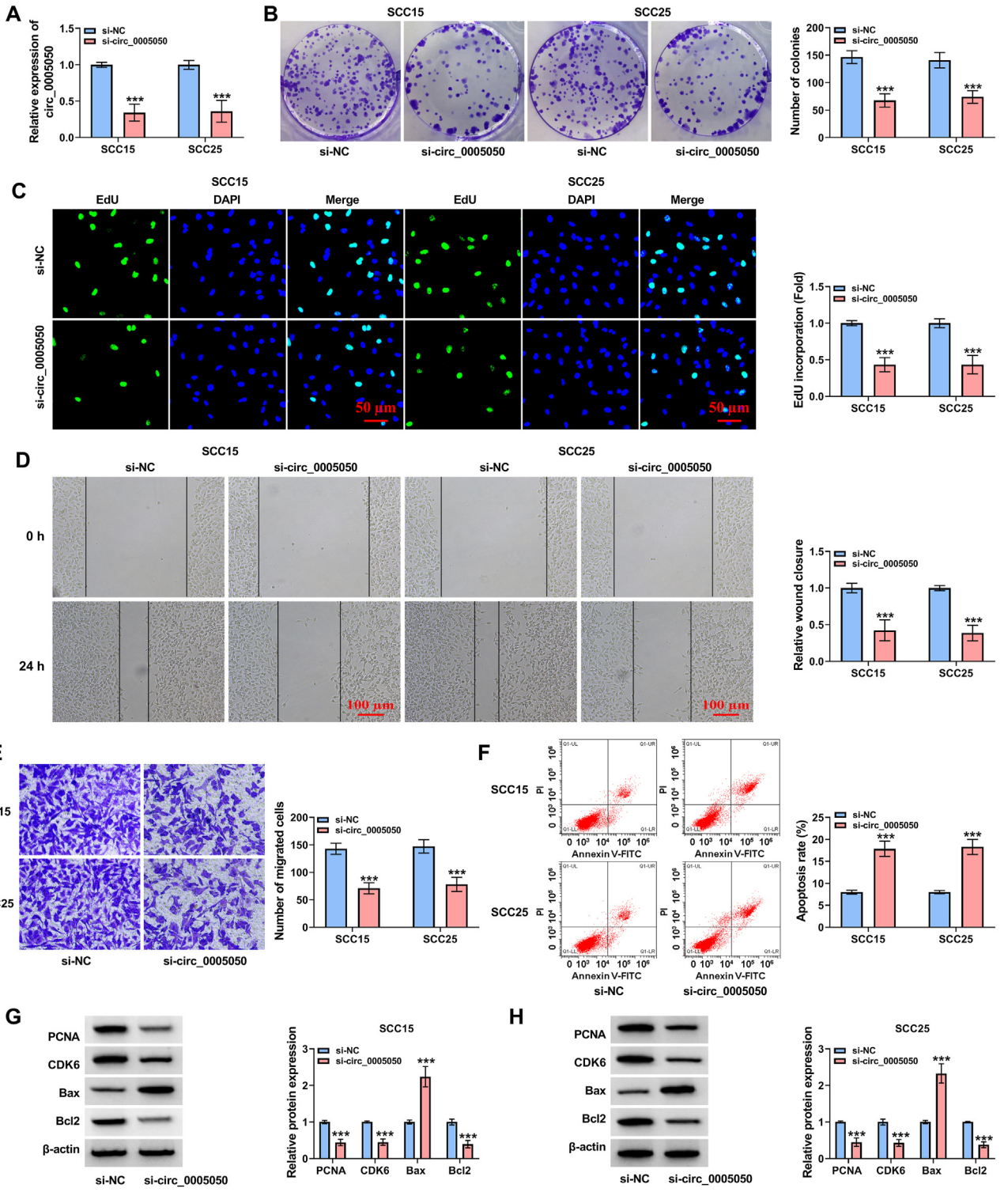

Fig. 2 Knockdown of circ_0005050 suppressed the malignant biological behavior of OSCC cells. (A) QRT-PCR was used to examine the expression of circ_0005050 in both SCC15 and SCC25 cells when transfected with si-circ_0005050 or si-NC. (B) Colony formation assay was used to evaluate the colony formation rate. (C) EdU assay was applied to evaluate cell proliferation. (D and E) The migration capacity of OSCC cells was tested using wound healing and Transwell assays. (F) Cell apoptosis was determined by flow cytometry assay. (G and H) Western blot was performed to measure the protein levels of PCNA, CDK6, Bax and Bcl2. ***$P < 0.001$.

tissues and cells (Fig. 5B–D). Luciferase activity of CHSY1 3′UTR was effectively decreased in SCC15 and SCC25 cells co-transfected with miR-487a-3p mimic (Fig. 5E and F). To further confirm the mutual effect of miR-487a-3p and CHSY1 at endogenous levels, we carried out RIP assay. As expected, we noticed that miR-487a-3p and CHSY1 were

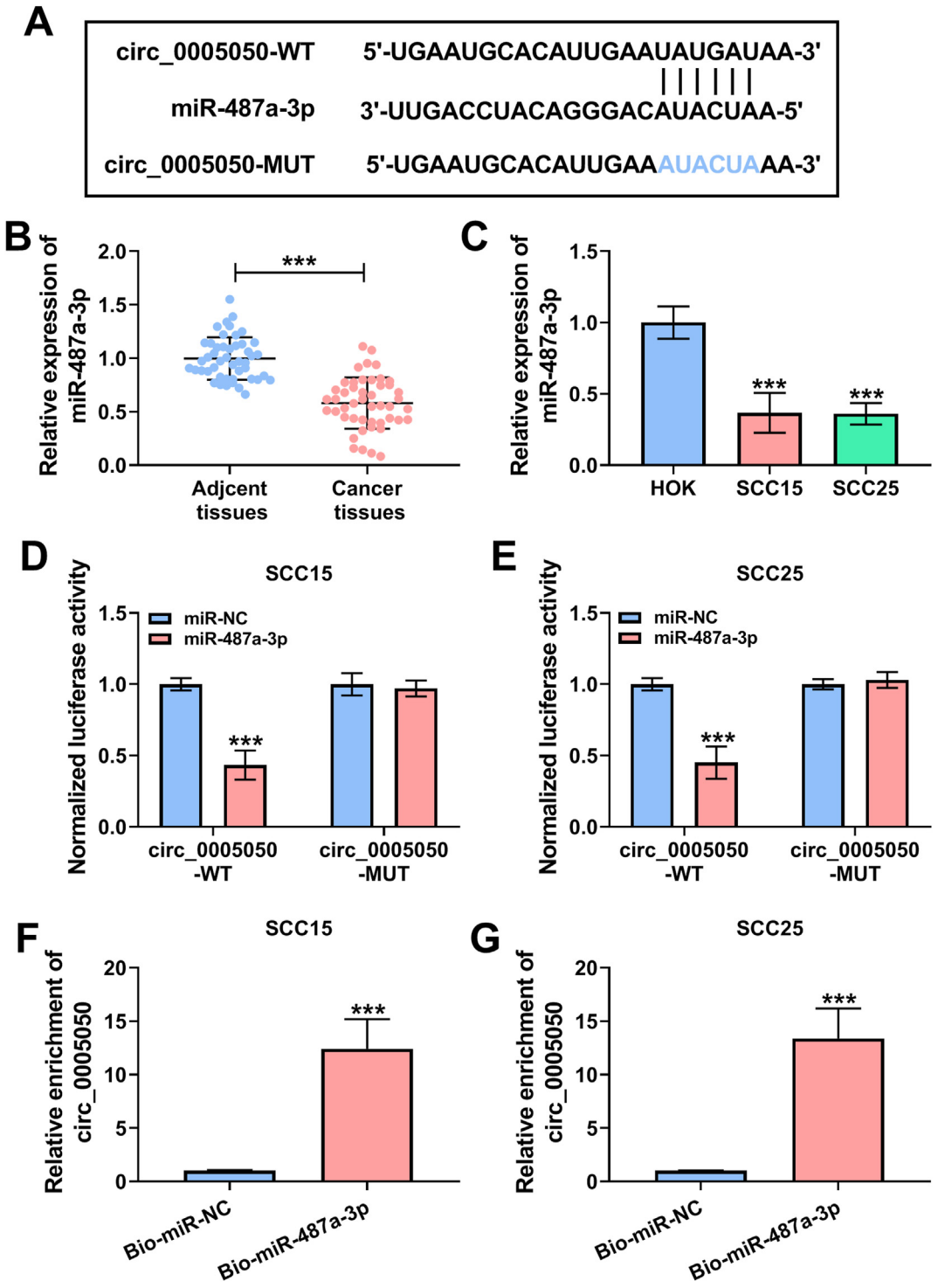

Fig. 3 Circ_0005050 functioned as a sponge of miR-487a-3p in OSCC cells. (A) The circinteractome algorithm showed the complementary binding sites between circ_0005050 and miR-487a-3p. (B and C) qRT-PCR measured miR-487a-3p level in OSCC tissues and cells. (D and E) Dual-luciferase reporter assay examined luciferase activity of SCC15 and SCC25 cells co-transfected with circ_0005050-WT/MUT and miR-487a-3p mimic or the negative control (miR-NC). (F and G) RNA pull-down assay measured circ_0005050 enrichment in cell extracts of SCC15 and SCC25 cells transfected with Bio-miR-487a-3p or Bio-miR-NC. ***$P < 0.001$.

apparently enriched in Ago2 pellets of SCC15 and SCC25 cell extracts relative to the IgG control group (Fig. S3). Additionally, CHSY1 protein expression was significantly upregulated in anti-miR-487a-3p group compared to anti-miR-NC group (Fig. 5G and H). Furthermore, Western blot data revealed that circ_0005050 silencing caused inhibition of CHSY1 expression in SCC15 and SCC25 cells, which was recovered by anti-miR-487a-3p addition (Fig. 5I and J).

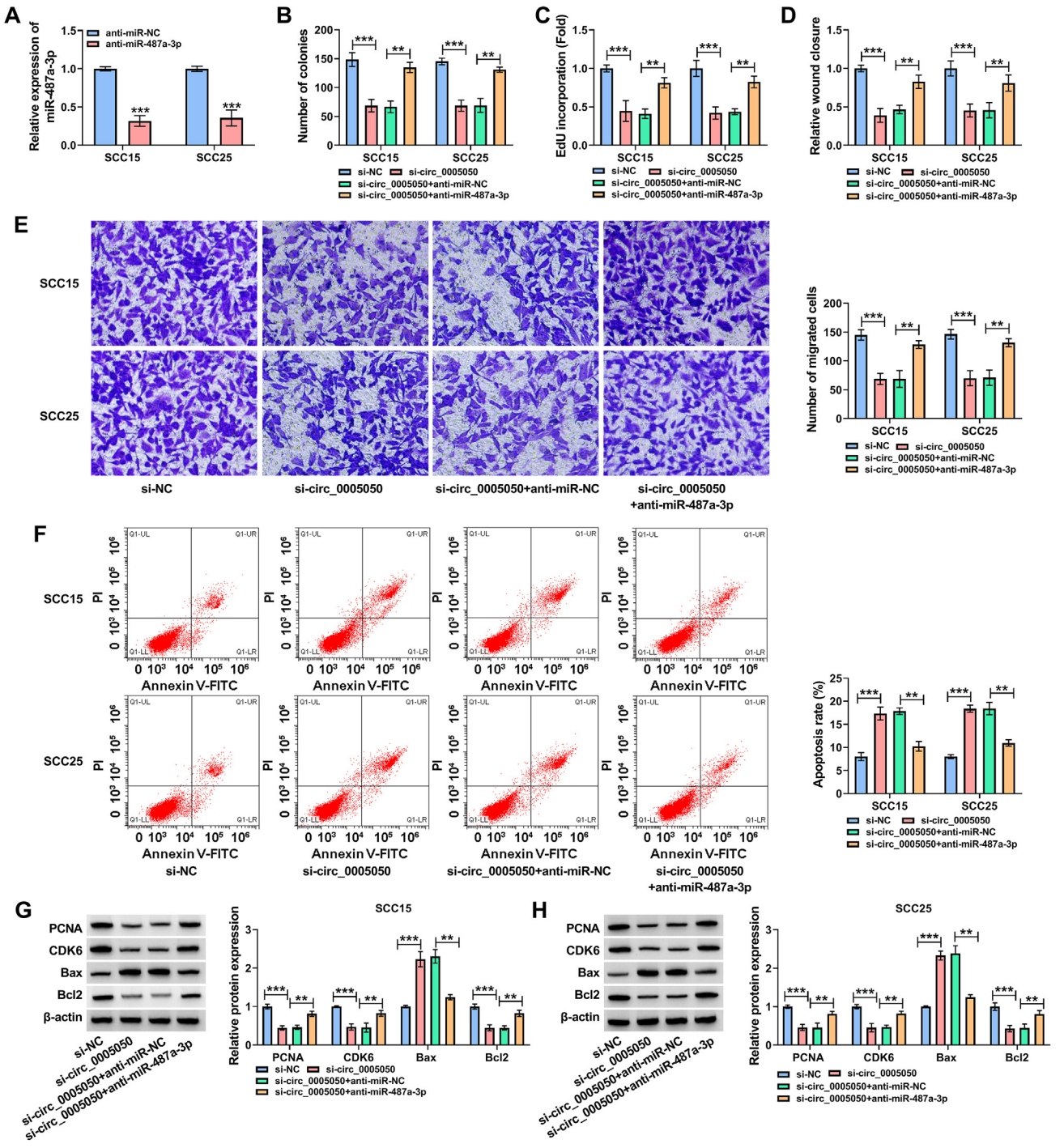

Fig. 4 Inhibition of miR-487a-3p reversed the role of circ_0005050 knockdown in SCC15 and SCC25 cells. (A) Transfection efficiency of anti-miR-487a-3p was detected by qRT-PCR. (B and C) Cell proliferation was monitored by colony formation and EdU assays. (D and E) Number of migrated cells was observed through the wound healing and transwell assays. (F) Cell apoptosis was assessed by flow cytometry assay. (G and H) Protein levels of PCNA, CDK6, Bax and Bcl2 were quantified by Western blot. $^{**}P < 0.01$, $^{***}P < 0.001$.

Furthermore, our results indicated that CHSY1 expression was positively correlated with circ_0005050 and inversely associated with miR-487a-3p in OSCC tissues samples (Fig. S2B and S2C). These results displayed a direct interaction between miR-487a-3p and CHSY1 in OSCC cells, moreover, circ_0005050 could regulate CHSY1 through miR-487a-5p.

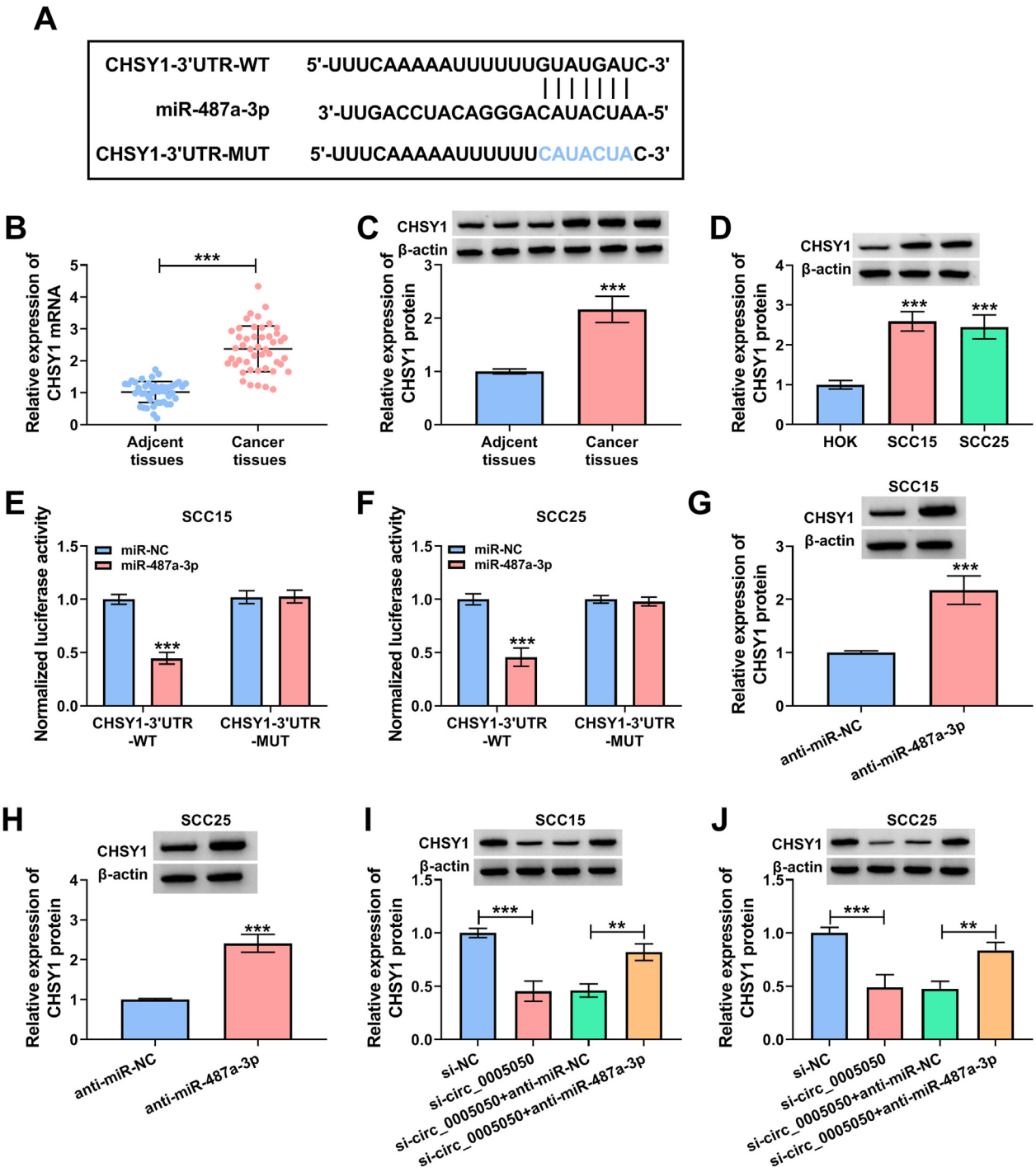

Fig. 5 The downstream target of miR-487a-3p in OSCC cells. (A) The starBase showed the complementary binding sites among CHSY1 3′UTR and miR-487a-3p. (B—D) QRT-PCR and Western blot assessed CHSY1 mRNA and protein expression in OSCC tissues and cell lines. (E and F) Dual-luciferase reporter assay examined luciferase activity of SCC15 and SCC25 cells co-transfected with CHSY1-3′UTR-WT/MUT and miR-487a-3p or miR-NC. (G and H) Western blot monitored CHSY1 protein expression in SCC15 and SCC25 cells. (I and J) Western blot evaluated CHSY1 protein level in SCC15 and SCC25 cells transfected with si-NC alone, si-circ_0005050 alone or together with anti-miR-487a-3p or anti-miR-NC. $^{**}P < 0.01$, $^{***}P < 0.001$.

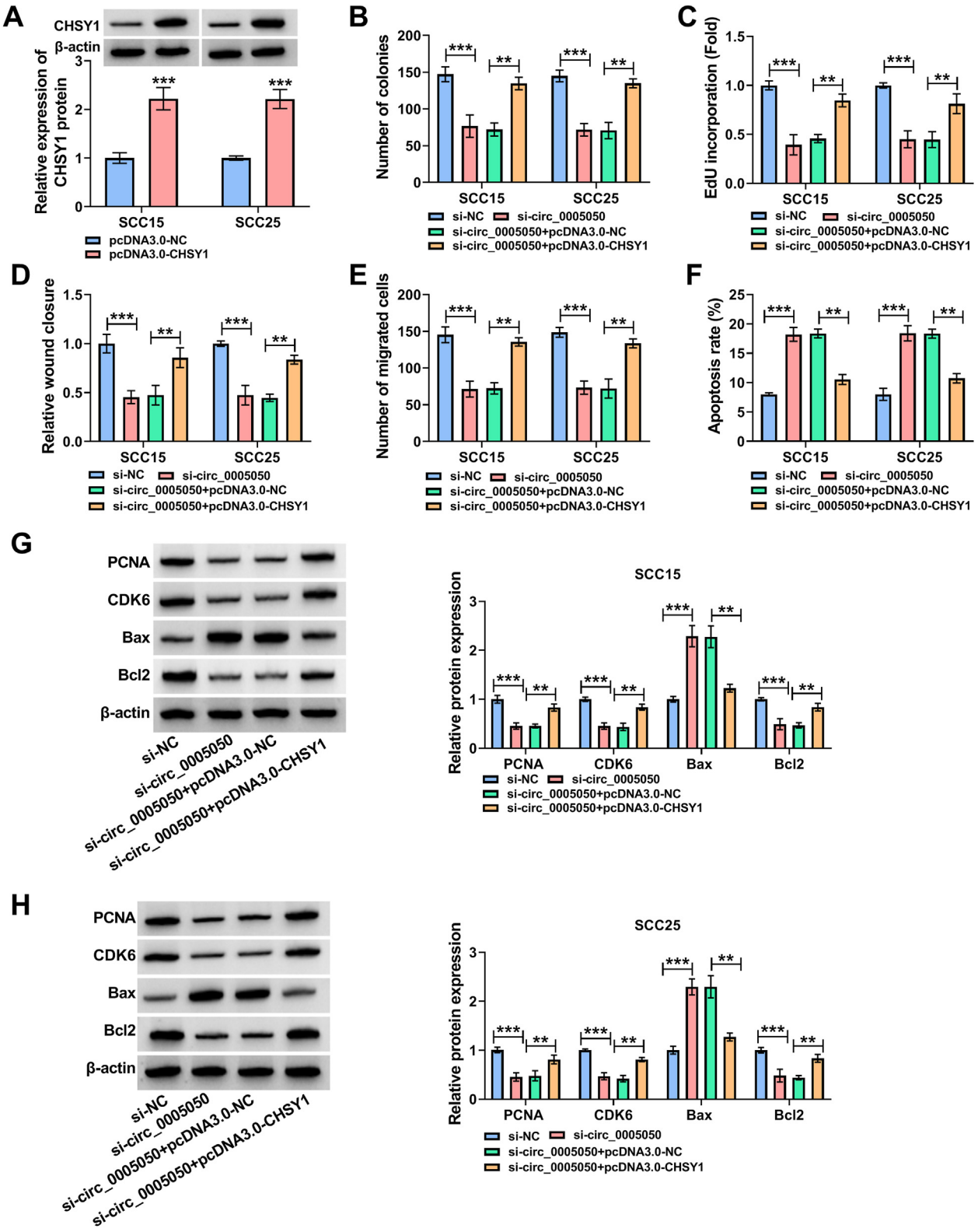

Fig. 6 Effects of CHSY1 overexpression on the progression of OSCC cells. (A) The protein level of CHSY1 in SCC15 and SCC25 cells were measured by Western blot analysis to evaluate the transfection efficiency of pcDNA3.0-CHSY1. (B and C) Colony formation and EdU assays were performed to assess cell proliferation. (D and E) Cell migration was detected by wound healing and transwell assays. (G and H) Western blot analysis was used to measure the protein levels of PCNA, CDK6, Bax and Bcl2. $^{**}P < 0.01$, $^{***}P < 0.001$.

Overexpression of CHSY1 recuperated the inhibition effect of si-circ_0005050 on the progression of OSCC

Prominent promotion of the CHSY1 protein level caused by pcDNA3.0-CHSY1 manifested that its transfection efficiency was good (Fig. 6A). Colony formation and EdU assays displayed that pcDNA3.0-CHSY1 could recede the inhibition of circ_0005050 silencing on cell proliferation (Fig. 6B and C). Wound healing and transwell assays revealed that si-circ_0005050 inhibited the migration of SCC15 and SCC25 cells, while this inhibition effect could be recovered by pcDNA3.0-CHSY1 (Fig. 6D and E). Through flow cytometry, we observed that circ_0005050 knockdown promoted OSCC cell apoptosis, while pcDNA3.0-CHSY1 attenuated this effect (Fig. 6F). Circ_0005050 knockdown inhibited PCNA, CDK6 and Bcl2 proteins expression, and promoted Bax protein levels, which were recovered by PCDNA3.0-CHSY1 (Fig. 6G and H). Therefore, these data verified that CHSY1 had an important role on the adjustment of the circ_0005050/miR-487a-3p axis in OSCC progression.

Knockdown of circ_0005050 restrained tumor growth of OSCC cells *in vivo*

In vivo, xenograft tumor models were utilized to measure tumor growth of SCC15 cells in nude mice. As shown in Fig. 7A and B, the volume and weight of xenograft tumors were impeded by sh-circ_0005050 transfection. Molecularly, sh-circ_0005050 transfection led to a downregulation of circ_0005050 and CHSY1 in xenograft tumors, as well as an upregulation of miR-487a-3p (Fig. 7C—E). ICH results showed that Ki-67 protein level was retarded in sh-circ_0005050 group (Fig. 7F). Moreover, our data suggested that the overexpression of circ_0005050 might improve tumor cell growth in xenograft tumors (Fig. S1C—E). These outcomes suggested a suppressive role of circ_0005050 knockdown in tumor growth.

Discussion

CircRNA was considered as a kind of gene splicing byproduct without practical effect in the early stage, and has now been found to be associated with a variety of human diseases, such as osteoarthritis;[22] autoimmune diseases,[23] etc. Studies have shown that circRNA can sponge the miRNA to prevent the inhibiting effect of miRNA on mRNA,[24] and circRNA can be used as a tumor biomarker.[25] CircRNA has become a popular research object in tumor research in recent years, and circRNA has played a significant role in the progression of tumors in gastric cancer,[26] osteosarcoma,[27] liver cancer,[28] and esophageal squamous cell carcinoma.[29] In OSCC, circ_0000140 has been shown to inhibit OSCC cell growth and metastasis by targeting miR-31.[30] Furthermore, a previous report suggested that

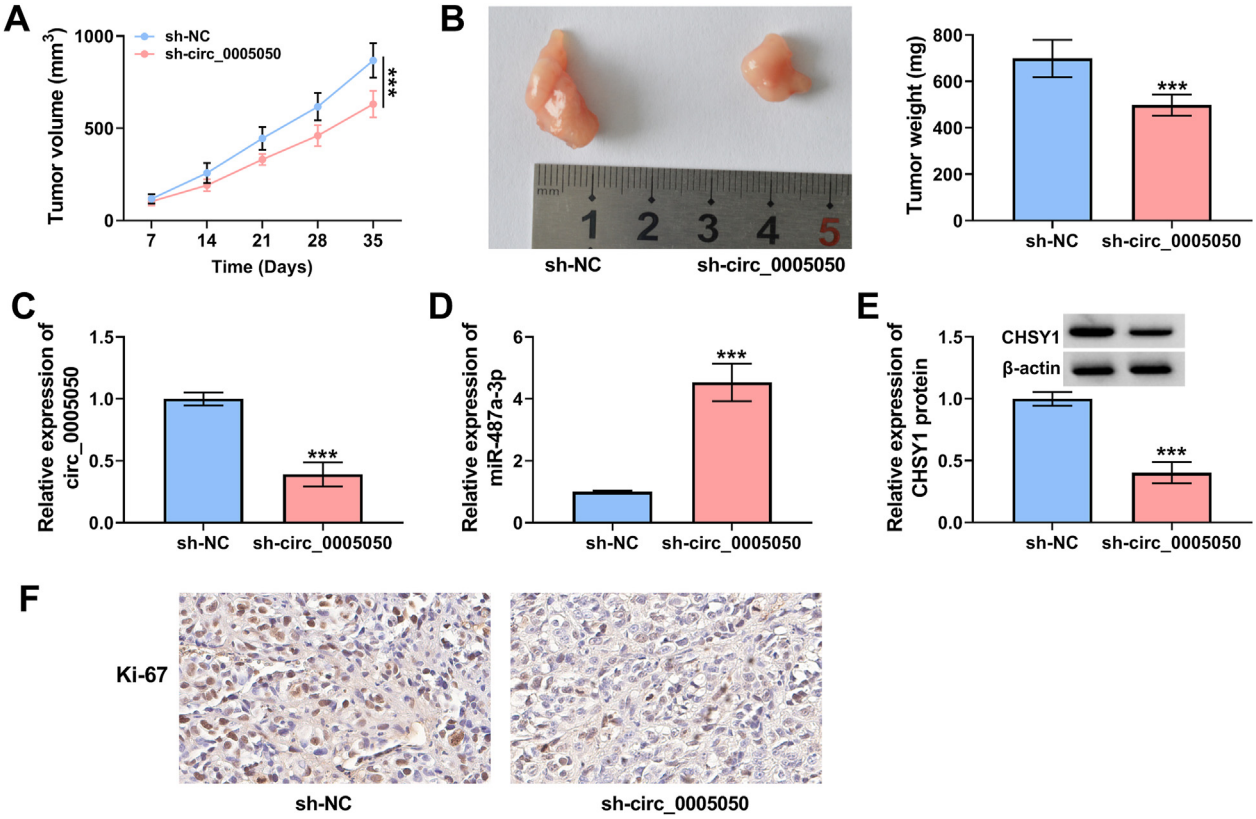

Fig. 7 Role of circ_0005050 of OSCC cells *in vivo*. (A and B) Tumor volume and weight were measured. (C and D) QRT-PCR measured circ_0005050 and miR-487a-3p levels in tumor tissues of xenograft mice. (E) Western blot measured CHSY1 protein level in tumor tissues of xenograft mice. (F) ICH estimated the expression of Ki-67. ***$P < 0.001$.

circ_0005050, a novel researched circRNA, was found with different expression in OSCC tissues and normal oral mucosal tissues,[31] but its function and mechanism remain obscure in OSCC. In this paper, circ_0005050 deriving from exons 17, 18, 19, and 20 of its host gene XPO1, was drastically increased in OSCC tissues and cell lines. Also, the silencing of circ_0005050 might relieve OSCC cell malignant behavioral phenotypes by repressing cell proliferative ability, migration, and inducing apoptosis. Consistently, the repression of circ_0005050 knockdown on tumor cell growth was also demonstrated in OSCC xenografts in nude mice. These results implied that circ_0005050 might be a promising predictive and therapeutic target for OSCC treatment.

CircRNA may be involved in regulating downstream mRNA expression through adsorption of miRNA.[32] Dual-luciferase reporter gene assay and RNA pull-down assay confirmed that circ_0005050 targeted miR-487a-3p. It has been widely proved that miR-487a-3p had frequent abnormal expression in a large number of human cancers, such as pancreatic cancer,[33] prostate cancer,[34] and non-small cell lung cancer.[35] Notably, some researchers have discovered the downregulation and viral impact of miR-487a-3p in OSCC. For example, miR-487a-3p functioned as a new tumor suppressor in OSCC through repressing tumor cell growth and invasion.[18] Meanwhile, the downregulation of miR-487a-3p might partly abolish the suppressive role of lncRNA TSPEAR-AS2 deficiency on OSCC cell proliferation, migration, and invasion *in vitro*.[36] Consistent with these former reports, the current work exhibited an apparent decrease of miR-487a-3p on OSCC tissue samples and cell lines. Furthermore, functional analysis indicated that the under-expressed miR-487a-3p might partially overturn circ_0005050 knockdown-mediated cell proliferation and migration inhibition, and apoptosis promotion in OSCC cells. The above findings suggested silencing of circ_0005050 might relieve OSCC cell malignant biological properties by sponging miR-487a-3p.

It has been acknowledged that miRNAs might modulate tumorigenesis through regulating their target mRNAs.[37,38] Using bioinformatics software and dual-luciferase reporter assay, CHSY1 was identified to be a direct target of miR-487a-3p. Also, our data suggested that miR-487a-3p was significantly correlated with the expression level of CHSY1 in tumor cell lines. As an enzyme responsible for the biosynthesis of chondroitin sulfate, CHSY1 has been reported to be involved in the regulation of the occurrence and development of various tumors.[19,20,39] Moreover, it has been confirmed that CHSY1 acted as a tumor promoter in OSCC by aggressing cell proliferation, migration, and invasion.[21] In agreement with this report, our data suggested that the CHSY1 level was obviously increased in OSCC tissues and cell lines. More importantly, our results exhibited that elevation of CHSY1 could rescue the inhibitory impact of circ_0005050 inhibition on OCSS cell progression, further supporting the circ_0005050/miR-487a-3p/CHSY1 axis.

In conclusion, this study suggested that circ_0005050 knockdown was expected to inhibit the progression of OSCC through regulating the miR-487a-3p/CHSY1 axis, which provided a meaningful experimental basis for the exploration of biomarkers for the diagnosis and treatment of OSCC and a new diagnostic and therapeutic idea for the treatment of OSCC.

Declaration of competing interests

The authors declare that they have no known competing financial interests or personal relationships that could have appeared to influence the work reported in this paper.

Acknowledgments

None.

Appendix A. Supplementary data

Supplementary data to this article can be found online at https://doi.org/10.1016/j.jds.2022.05.012.

References

1. Ferlay J, Colombet M, Soerjomataram I, et al. Estimating the global cancer incidence and mortality in 2018: GLOBOCAN sources and methods. *Int J Cancer* 2019;144:1941–53.
2. Leemans CR, Snijders PJF, Brakenhoff RH. Publisher correction: the molecular landscape of head and neck cancer. *Nat Rev Cancer* 2018;18:662.
3. Ettinger KS, Ganry L, Fernandes RP. Oral cavity cancer. *Oral Maxillofac Surg Clin* 2019;31:13–29.
4. Siegel RL, Miller KD, Jemal A. Cancer statistics, 2019. *CA A Cancer J Clin* 2019;69:7–34.
5. Okano S, Homma A, Kiyota N, et al. Induction chemotherapy in locally advanced squamous cell carcinoma of the head and neck. *Jpn J Clin Oncol* 2021;51:173–9.
6. Maubec E. Update of the management of cutaneous squamous-cell carcinoma. *Acta Derm Venereol* 2020;100:adv00143.
7. Rapado-Gonzalez O, Martinez-Reglero C, Salgado-Barreira A, Lopez-Lopez R, Suarez-Cunqueiro MM, Muinelo-Romay L. miRNAs in liquid biopsy for oral squamous cell carcinoma diagnosis: systematic review and meta-analysis. *Oral Oncol* 2019;99:104465.
8. Yao C, Chang EI, Lai SY. Contemporary approach to locally advanced oral cavity squamous cell carcinoma. *Curr Oncol Rep* 2019;21:99.
9. Kristensen LS, Andersen MS, Stagsted LVW, Ebbesen KK, Hansen TB, Kjems J. The biogenesis, biology and characterization of circular RNAs. *Nat Rev Genet* 2019;20:675–91.
10. Patop IL, Wust S, Kadener S. Past, present, and future of circRNAs. *EMBO J* 2019;38:e100836.
11. Salzman J, Gawad C, Wang PL, Lacayo N, Brown PO. Circular RNAs are the predominant transcript isoform from hundreds of human genes in diverse cell types. *PLoS One* 2012;7:e30733.
12. Zhang HD, Jiang LH, Sun DW, Hou JC, Ji ZL. CircRNA: a novel type of biomarker for cancer. *Breast Cancer* 2018;25:1–7.
13. Patop IL, Kadener S. circRNAs in cancer. *Curr Opin Genet Dev* 2018;48:121–7.
14. Zhu X, Du J, Gu Z. Circ-PVT1/miR-106a-5p/HK2 axis regulates cell growth, metastasis and glycolytic metabolism of oral squamous cell carcinoma. *Mol Cell Biochem* 2020;474:147–58.
15. Michlewski G, Caceres JF. Post-transcriptional control of miRNA biogenesis. *RNA* 2019;25:1–16.
16. He B, Zhao Z, Cai Q, et al. miRNA-based biomarkers, therapies, and resistance in cancer. *Int J Biol Sci* 2020;16:2628–47.
17. Zhang HY, Ma JH. MiR-105 promotes the progression and predicts the prognosis for oral squamous cell carcinoma (oscc). *Cancer Manag Res* 2020;12:11491–9.
18. Wang L, Ge S, Zhou F. MicroRNA-487a-3p inhibits the growth and invasiveness of oral squamous cell carcinoma by targeting PPM1A. *Bioengineered* 2021;12:937–47.

19. Zeng L, Qian J, Luo X, Zhou A, Zhang Z, Fang Q. CHSY1 promoted proliferation and suppressed apoptosis in colorectal cancer through regulation of the NFkappaB and/or caspase-3/7 signaling pathway. *Oncol Lett* 2018;16:6140—6.
20. Liu CH, Lan CT, Chou JF, Tseng TJ, Liao WC. CHSY1 promotes aggressive phenotypes of hepatocellular carcinoma cells via activation of the hedgehog signaling pathway. *Cancer Lett* 2017;403:280—8.
21. Li J, Xu X, Zhang D, Lv H, Lei X. Lncrna lhfpl3-as1 promotes oral squamous cell carcinoma growth and cisplatin resistance through targeting mir-362-5p/chsy1 pathway. *OncoTargets Ther* 2021;14:2293—300.
22. Wu Y, Zhang Y, Zhang Y, Wang JJ. CircRNA hsa_circ_0005105 upregulates NAMPT expression and promotes chondrocyte extracellular matrix degradation by sponging miR-26a. *Cell Biol Int* 2017;41:1283—9.
23. Cardamone G, Paraboschi EM, Rimoldi V, Duga S, Solda G, Asselta R. The characterization of gsdmb splicing and backsplicing profiles identifies novel isoforms and a circular rna that are dysregulated in multiple sclerosis. *Int J Mol Sci* 2017;18:576.
24. Momen-Heravi F, Bala S. Emerging role of non-coding RNA in oral cancer. *Cell Signal* 2018;42:134—43.
25. Zhu M, Xu Y, Chen Y, Yan F. Circular BANP, an upregulated circular RNA that modulates cell proliferation in colorectal cancer. *Biomed Pharmacother* 2017;88:138—44.
26. Li C, Li M, Xue Y. Downregulation of CircRNA CDR1as specifically triggered low-dose diosbulbin-B induced gastric cancer cell death by regulating miR-7-5p/REGgamma axis. *Biomed Pharmacother* 2019;120:109462.
27. Li B, Li X. Overexpression of hsa_circ_0007534 predicts unfavorable prognosis for osteosarcoma and regulates cell growth and apoptosis by affecting AKT/GSK-3beta signaling pathway. *Biomed Pharmacother* 2018;107:860—6.
28. Xie B, Zhao Z, Liu Q, Wang X, Ma Z, Li H. CircRNA has_circ_0078710 acts as the sponge of microRNA-31 involved in hepatocellular carcinoma progression. *Gene* 2019;683:253—61.
29. Cao S, Chen G, Yan L, Li L, Huang X. Contribution of dysregulated circRNA_100876 to proliferation and metastasis of esophageal squamous cell carcinoma. *OncoTargets Ther* 2018;11:7385—94.
30. Peng QS, Cheng YN, Zhang WB, Fan H, Mao QH, Xu P. circRNA_0000140 suppresses oral squamous cell carcinoma growth and metastasis by targeting miR-31 to inhibit Hippo signaling pathway. *Cell Death Dis* 2020;11:112.
31. Zhang S, Han J, Fu J. The circ_0032822 promotes the proliferation of head and neck squamous cell carcinoma cells through mir-141/ef3 signaling axis. *Front Oncol* 2021;11:662496.
32. Hansen TB, Jensen TI, Clausen BH, et al. Natural RNA circles function as efficient microRNA sponges. *Nature* 2013;495:384—8.
33. Zhou J, Qie S, Fang H, Xi J. MiR-487a-3p suppresses the malignant development of pancreatic cancer by targeting SMAD7. *Exp Mol Pathol* 2020;116:104489.
34. Yu L, Ren Y. Long Noncoding rna small nucleolar rna host gene 3 mediates prostate cancer migration, invasion, and epithelial-mesenchymal transition by sponging mir-487a-3p to regulate trim25. *Cancer Biother Radiopharm* 2021. https://doi.org/10.1089/cbr.2020.3988.
35. Fan Y, Hao J, Cen X, et al. Downregulation of miR-487a-3p suppresses the progression of non-small cell lung cancer via targeting Smad7. *Drug Dev Res* 2021. https://doi.org/10.1002/ddr.21876.
36. Xia YC, Cao J, Yang J, Zhang Y, Li YS. Lncrna tspear-as2, a novel prognostic biomarker, promotes oral squamous cell carcinoma progression by upregulating ppm1a via sponging mir-487a-3p. *Dis Markers* 2021;2021:2217663.
37. Di Leva G, Garofalo M, Croce CM. MicroRNAs in cancer. *Annu Rev Pathol* 2014;9:287—314.
38. Mokhtaridoost M, Gonen M. An efficient framework to identify key miRNA-mRNA regulatory modules in cancer. *Bioinformatics* 2020;36:i592—600.
39. Liu J, Tian Z, Liu T, et al. CHSY1 is upregulated and acts as tumor promotor in gastric cancer through regulating cell proliferation, apoptosis, and migration. *Cell Cycle* 2021;20:1861—74.